THz absorption spectrum of the CO2–H2O complex: Observation and assignment of intermolecular van der Waals vibrations

Andersen, Jonas; Heimdal, J.; Wallin Mahler Andersen, Denise; Nelander, B.; Larsen, René Wugt

Published in:
Journal of Chemical Physics

Link to article, DOI:
10.1063/1.4867901

Publication date:
2014

Document Version
Publisher's PDF, also known as Version of record

Communication: THz absorption spectrum of the CO_2–H_2O complex: Observation and assignment of intermolecular van der Waals vibrations

J. Andersen,[1] J. Heimdal,[2] D. W. Mahler,[1] B. Nelander,[2] and R. Wugt Larsen[1,a)]
[1]*Department of Chemistry, Technical University of Denmark, Kemitorvet 206, 2800 Kgs. Lyngby, Denmark*
[2]*MAX-IV Laboratory, Lund University, P. O. Box 118, 22100 Lund, Sweden*

(Received 4 February 2014; accepted 25 February 2014; published online 7 March 2014)

Terahertz absorption spectra have been recorded for the weakly bound CO_2–H_2O complex embedded in cryogenic neon matrices at 2.8 K. The three high-frequency van der Waals vibrational transitions associated with out-of-plane wagging, in-plane rocking, and torsional motion of the isotopic H_2O subunit have been assigned and provide crucial observables for benchmark theoretical descriptions of this systems' flat intermolecular potential energy surface. A (semi)-empirical value for the zero-point energy of 273 ± 15 cm^{-1} from the class of intermolecular van der Waals vibrations is proposed and the combination with high-level quantum chemical calculations provides a value of 726 ± 15 cm^{-1} for the dissociation energy D_0. © *2014 AIP Publishing LLC*. [http://dx.doi.org/10.1063/1.4867901]

The intermolecular interaction between CO_2 and H_2O plays a major role for a variety of phenomena in physics, chemistry, and biology including the radiative transfer through the Earth's and other planetary atmospheres,[1] the early stages in carbonic acid formation[2] and the transportation of dissolved CO_2 in the tissues of biological organisms. The prototypical binary mixed van der Waals complex of CO_2 and H_2O has been intensively investigated by both theory and experiment. Numerous quantum-chemical studies of the systems' intermolecular potential energy surface (IPES) have been reported.[3–13] High level of electron correlation, extensive basis sets, and inclusion of basis set superposition errors prove mandatory as the IPES is extremely flat near the global potential energy minimum. A recent comprehensive work reports a complete 5D *ab initio* IPES composed of 23 000 high level single-point energies in configuration space and settles that the global potential energy minimum has a planar and T-shaped geometry of C_{2v} symmetry with the oxygen atom of H_2O bound to the C atom and the H atoms pointing away from the CO_2 molecule[14] (Fig. 1). This global potential energy minimum geometry has independently been confirmed experimentally by a variety of spectroscopic studies[15–17,27] whereas other works have suggested the existence of other higher energy configurations.[18,19] The most important observable is the dissociation energy D_0 which requires reliable band origins for the system's complete set of fundamental vibrational transitions and in particular for the class of five intermolecular van der Waals vibrational transitions addressed in the present work.

Neon (L'Air Liquide, 99.5%) doped with CO_2 (Matheson, 99.9%) and degassed samples of H_2O, $H_2{}^{18}O$ (Sigma Aldrich, 99.0% ^{18}O) and D_2O (Sigma Aldrich, 99.5% D) with mixing ratios of ≃0.5‰ to 5‰ were deposited with a flow rate of 0.02 mol/h at 3.6 K on a gold-plated oxygen-free high thermal conductivity (OFHC) copper mirror inside an immersion helium cryostat (IHC-3) modified for matrix isolation spectroscopy at MAX-lab.[20] A 3-mm deep cavity with 10-mm diameter and a flat bottom has been drilled into the mirror centre to allow deposition of several millimeter thick matrices doped with weak absorbers. The mirror temperature was monitored by a Lake Shore silicon diode and maintained stable at 2.8 ± 0.1 K before and after deposition employing resistive heaters and feedback electronics. The sample mount was equipped with interchangeable CsI and polymethylpentene (TPX) windows and combined IR and THz single-beam spectra were collected by a Bruker IFS 120 FTIR spectrometer employing a globar lamp as radiation source. A HgCdTe detector combined with a Ge/KBr beam splitter and a Si-bolometer operating at 4.2 K combined with a 6 μm multilayer Mylar beam splitter were employed for the IR and THz spectral regions, respectively. Spectral resolutions of 0.1–1 cm^{-1} were selected depending on the observed bandwidths.

Figure 2 shows a series of THz absorption spectra collected for several millimeter thick cryogenic neon matrices doped with CO_2 (CO_2:H_2O:Ne)=(1:0:800), H_2O (0:1:4000), and mixtures of CO_2 and H_2O (3:1:4000), respectively. A

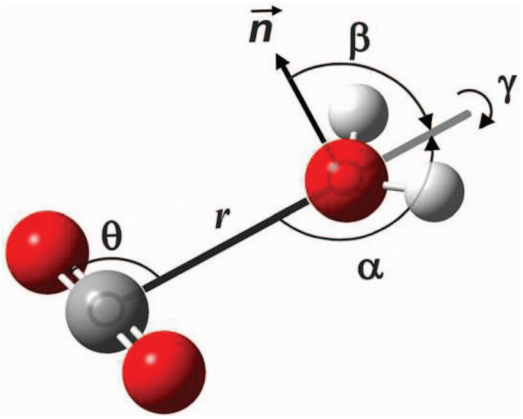

FIG. 1. The five intermolecular coordinates (r,α,β,γ,θ) specifying the configuration of the CO_2–H_2O van der Waals complex.

a)Author to whom correspondence should be addressed. Electronic mail: rewl@kemi.dtu.dk

dominant spectral feature observed for the matrices doped with regular H_2O is observed at 79.5 cm^{-1}. This band has previously been assigned to a rotational-translation-coupling (RTC) transition of H_2O monomer in neon[21] and helps to monitor the H_2O monomer concentration. At higher H_2O concentrations, signs of hydrogen-bonded dimers of water started to show up. The strongest intermolecular hydrogen bond vibrations of $(H_2O)_2$ observed in the THz region, the acceptor torsional and acceptor wagging modes, have previously been observed and assigned in neon matrices at 116.0 cm^{-1} and 122.2 cm^{-1}.[20,22–24] THz spectra recorded for neon matrices doped solely with CO_2 showed no signs of CO_2-containing cluster entities in agreement with high-level theoretical studies of the weakly bound $(CO_2)_2$ system.[25] As shown in Fig. 2 the simultaneous use of CO_2 and H_2O as dopants allowed the identification of two new distinct bands located at 101.6 and 166.6 cm^{-1}; the latter band being a factor of 3–4 less intense. The intensity of these bands increased similarly with the CO_2 and H_2O concentration suggesting the assignments to a mixed $(CO_2)_n$–$(H_2O)_n$ complex. A stoichiometric 1:1 relationship could be confirmed at the low sample concentrations and by the complementary IR spectral series. THz spectra collected for neon matrices doped with CO_2 and isotopically enriched samples of $H_2{}^{18}O$ and D_2O/HDO are useful to validate the proposed assignments further. An illustrative spectrum obtained for $CO_2/H_2{}^{18}O$ doped neon matrices is shown in Fig. 2. The small isotopic shifts upon ^{18}O-substitution have been reported previously both for the monomeric RTC transition[21] and the strongest dimeric hydrogen bond vibrations of water.[20] The observed spectral shifts caused by the ^{18}O-substitution are also very small for both the proposed CO_2–H_2O bands. The band at 101.6 cm^{-1} seems to be rather unaffected by the ^{18}O-substitution. The upper band has a small but significant reproducible isotopic red-shift of 1.9 cm^{-1} as indicated by arrows in Fig. 2. The effect of deuteration has a much larger impact on the recorded THz spectra since both the monomeric and dimeric water spectral features have significant isotope shifts not to mention that mixed isotopic entities start to build up. Both the D_2O and HDO as well as the mixed deuterated dimeric entities of water have been extensively studied previously and the complete list of spectral assignments is given in Table I. In the further spectral analysis of the isotopically enriched spectral signatures we consult quantum chemical predictions.

As described and cited in the introduction, a variety of high-level quantum chemical calculations have been performed to describe the accurate IPES of the CO_2–H_2O complex in great detail. In Table II, we have listed harmonic MP2/aug-cc-pVQZ predictions for the global potential energy

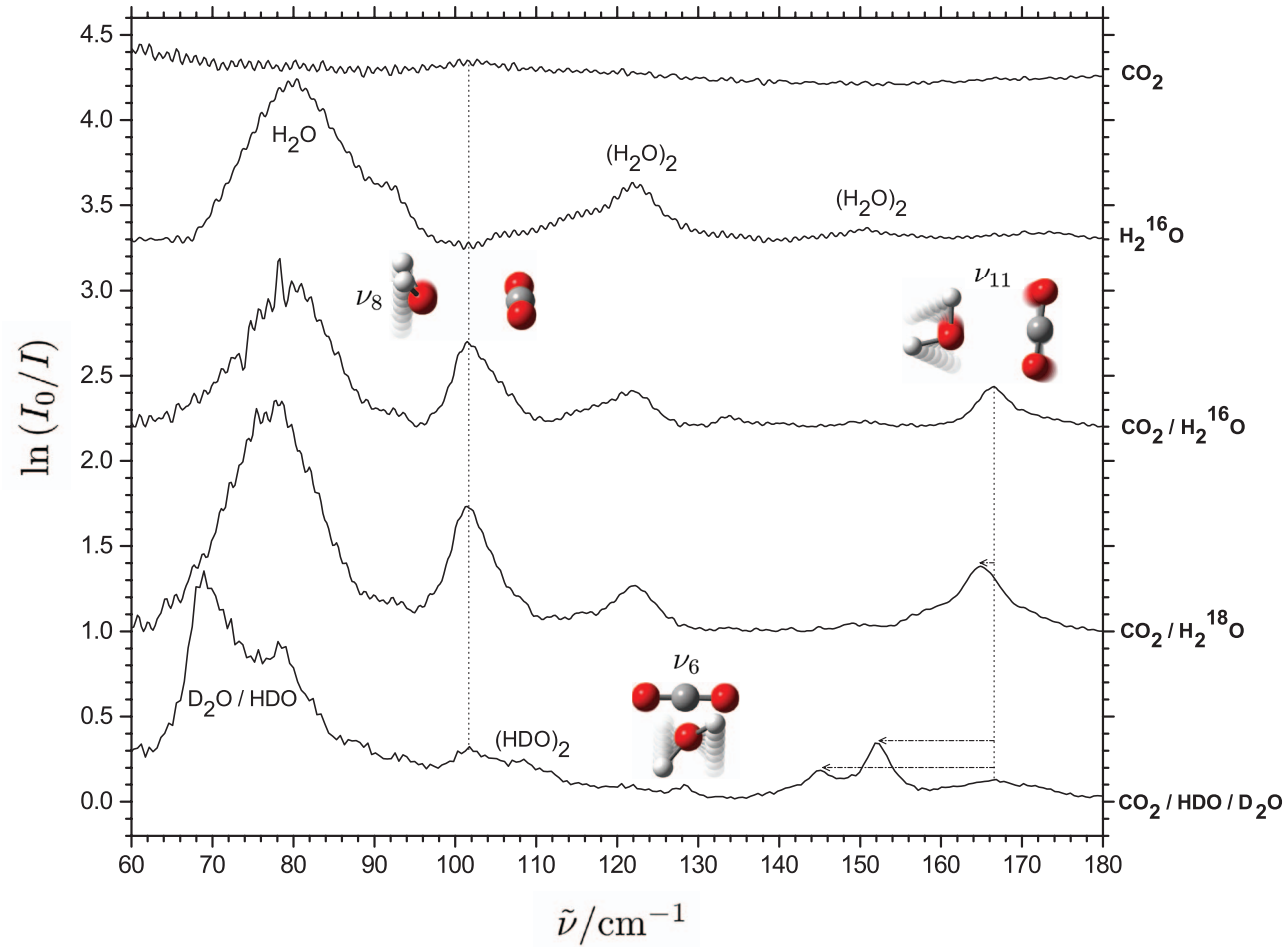

FIG. 2. A series of THz absorption spectra of 1.0 cm^{-1} resolution collected for cryogenic neon matrices doped with CO_2, H_2O, and 3:1 mixtures of CO_2 and isotopically enriched samples of H_2O at 2.8 K. The CO_2–H_2O assignments are indicated by animated normal vibrations.

TABLE I. The assigned transitions (units of cm^{-1}) for the recorded THz absorption spectra of $CO_2/H_2{}^{16}O$, $CO_2/H_2{}^{18}O$, CO_2/HDO, and CO_2/D_2O embedded in neon matrices at 2.8 K.

$CO_2/H_2{}^{16}O$	$CO_2/H_2{}^{18}O$	CO_2/HDO	CO_2/D_2O	Assignment
79.5[a]	77.8[a]		73.1[a]	H_2O monomer, RTC transition[a]
101.6[b]	**101.4**[b]			**CO_2–H_2O complex, H_2O wagging**
116.0[c]	116.0[c]			$(H_2O)_2$ complex, acceptor torsion
122.2[c]	122.0[c]	106.0[c]	93.3[c]	$(H_2O)_2$ complex, acceptor wagging
		128.4[b]		**CO_2–H_2O complex, H_2O torsion**
150.6[c]	149.7[c]	135.0[c]	123.1[c]	$(H_2O)_2$ complex, acceptor twist
166.6[b]	**164.7**[b]	**152.1**[b]	**145.1**[b]	**CO_2–H_2O complex, H_2O rocking**

[a]Rotation-translation-coupling transition (see Ref. 21).
[b]Present work.
[c]Reference 20.

minimum with C_{2v} symmetry. These predictions are in accordance with the study by Makarewicz[14] and specify the class of five intermolecular van der Waals vibrational transitions. The out-of-plane H_2O wagging mode ν_8 (B_1) described by the intermolecular coordinate β (Fig. 1) has a high intensity whereas the in-plane rocking of H_2O ν_{11} (B_2) described by α and the CO_2 librational rocking mode of ν_{12} (B_2) described by θ both have medium intensity. The H_2O torsional mode ν_6 (A_2) described by γ is strictly IR-forbidden for the regular CO_2–H_2O complex and the intermolecular O···C stretching mode ν_5 (A_1) described by r has a very low intensity. A convincing correlation immediately appears between the harmonic predictions and the observation of the two distinct bands at 101.6 and 166.6 cm^{-1} for THz spectra of neon matrices doped simultaneously with CO_2 and H_2O. This excellent agreement between experiment and theory suggests straightforward assignments for the out-of-plane H_2O wagging mode ν_8 at 101.6 cm^{-1} and the in-plane H_2O rocking mode ν_{11} at 166.6 cm^{-1} for the regular CO_2–H_2O complex. This agreement could partly be due to some kind of fortunate cancelation of smaller spectral shifts in opposite directions originating from anharmonicity effects and minor matrix perturbations which shall be discussed below. Small isotopic red-shifts are expected upon ^{18}O-substitution on the water subunit since both these intermolecular vibrational modes involve hindered rotational motion of H_2O. The harmonic calculations for the enriched CO_2–$H_2{}^{18}O$ system predict a very small red-shift of 0.9 cm^{-1} for the H_2O wagging mode ν_8 and a more pronounced red-shift of 2.2 cm^{-1} for the H_2O rocking mode ν_{11} (Table III). These red-shift predictions are convincingly close to the observations within the experimental reproducibility. The predicted relative harmonic band intensity agrees qualitatively with the experimental findings. The rotational motion of D_2O is much slower relative to H_2O and rather large isotopic spectral red-shifts for both the D_2O wagging and rocking modes are expected. The harmonic calculations for CO_2–D_2O accordingly predict red-shifts of 24.3 and 19.1 cm^{-1} with factors of 2 and 3 smaller harmonic band intensities, respectively, for these intermolecular van der Waals modes (Table III). The band origin for the strongest D_2O wagging mode is expected at 77.4 cm^{-1} and thereby unavoidably overlapped with the strong RTC transitions for H_2O, HDO, and D_2O (Table I). The band origin for the D_2O rocking mode with medium intensity is predicted at 148.5 cm^{-1} but the threefold loss of band intensity (8.5 km/mol) and the experimental challenge with isotopic H/D exchange and formation of HDO in the matrix inlet system was expected to blur this spectral signature. Nevertheless, a series of THz spectra recorded for neon matrices doped with CO_2/HDO/D_2O mixtures reproduces a medium strong band at 145.1 cm^{-1} which we assign to the D_2O rocking transition of the CO_2–D_2O complex as indicated in Fig. 2. The rotational motion of HDO is slower relative to H_2O but faster relative to D_2O and smaller predicted isotopic spectral red-shifts for the H_2O wagging and rocking modes of 18.1 and 11.6 cm^{-1}, respectively, for CO_2–HDO relative to CO_2–H_2O are both expected. The harmonic band intensities are both predicted to be a factor of 2 smaller for this isotopic variant of the complex. The band origin for the stronger HDO wagging mode predicted at 83.6 cm^{-1} cannot be observed unambiguously due to the overlapping RTC transitions of H_2O, HDO, and D_2O. The red-shifted HDO rocking mode predicted at 156.0 cm^{-1} with 14.5 km/mol intensity is easily observed and assigned at 152.1 cm^{-1} for the CO_2/HDO/D_2O doped neon matrices.

TABLE II. MP2/aug-cc-pVQZ predictions in the double harmonic approximation of vibrational band origins (units of cm^{-1}) and corresponding infrared band strengths (units of km/mol, in parenthesis) for the weakly bound CO_2–H_2O complex of C_{2v} symmetry.

Mode	Description	Origin (Int.)	Mode	Description	Origin (Int.)
ν_1 (A_1)	Sym. H_2O stretch	3836.3 (10)	ν_7 (B_1)	Out-of-plane CO_2 bend	667.2 (22)
ν_2 (A_1)	In-plane H_2O bend	1630.2 (76)	ν_8 (B_1)	Intermol. H_2O wagging	101.7 (228)
ν_3 (A_1)	Sym. CO_2 stretch	1334.7 (0.2)	ν_9 (B_2)	Antisym. H_2O stretch	3962.3 (87)
ν_4 (A_1)	In-plane CO_2 bend	653.2 (39)	ν_{10} (B_2)	Antisym. CO_2 stretch	2415.3 (564)
ν_5 (A_1)	Intermol. O···C stretch	111.2 (0.4)	ν_{11} (B_2)	Intermol. H_2O rocking	167.6 (25)
ν_6 (A_2)	Intermol. H_2O torsion	151.2 (0.0)	ν_{12} (B_2)	Intermol. CO_2 libration	16.8 (29)

TABLE III. Harmonic MP2/aug-cc-pVQZ predictions of vibrational band origins (units of cm^{-1}) and corresponding infrared band strengths (units of km/mol, in parenthesis) for the H_2O wagging, rocking, and torsional modes of different CO_2–H_2O isotopomers (the labeling refers to CO_2–$H_2{}^{16}O$).

Mode	Description	CO_2–$H_2{}^{16}O$	CO_2–$H_2{}^{18}O$	CO_2/HDO	CO_2/D_2O
ν_6 (A_2)	Intermol. H_2O torsion (γ)	151.2 (0)	151.2 (0)	135.9 (43)	108.3 (0)
ν_8 (B_1)	Intermol. H_2O wagging (β)	101.7 (228)	100.8 (225)	83.6 (133)	77.4 (125)
ν_{11} (B_2)	Intermol. H_2O rocking (α)	167.6 (25)	165.4 (25)	156.0 (14)	148.5 (9)

This assignment is indicated in Fig. 2 for an experiment with a CO_2:D_2O:HDO:H_2O composition of (18:6:6:1). The harmonic calculations of CO_2–HDO predict that the HDO torsional mode becomes IR-active. A band origin for the IR-forbidden H_2O torsional mode is predicted at 151.2 cm^{-1} for regular CO_2–H_2O and red-shifted to 135.9 cm^{-1} with significant intensity for the isotopic CO_2–HDO variant of C_s symmetry. The spectral series of CO_2/HDO/D_2O doped neon matrices confirms another weaker band at 128.4 cm^{-1} (Fig. 2) which does not show up in neon matrices doped solely with HDO/D_2O. This indirect and so far tentative assignment for the IR-forbidden H_2O torsional mode ν_6 for the regular CO_2–H_2O complex requires extra attention in the discussion of this transition's contribution to the zero-point energy.

The present experimental findings for the weakly bound CO_2–H_2O system enable us to provide a (semi)-empirical estimate of the system's zero-point energy. The weakly bound nature of the CO_2–H_2O system results in rather small perturbations of the intramolecular vibrational transitions. The total shift of the zero-point energy contribution to D_0 caused by perturbations of intramolecular vibrational transitions is in the order of 5 cm^{-1}.[14] A reliable determination of the system's zero-point energy thus relies completely on accurate band origins for the set of five intermolecular van der Waals vibrational transitions introduced by complex formation. According to our harmonic MP2 predictions, the three observed transitions constitute about 75% of the total intermolecular vibrational zero-point energy contribution to the dissociation energy D_0. The contributions from the H_2O wagging mode ν_8 observed at 101.6 cm^{-1} and the H_2O rocking mode ν_{11} observed at 166.6 cm^{-1} are clear. In order to establish the contribution from the IR-forbidden H_2O torsional mode ν_6 we consider the effect of H/D substitution on this kind of motion. The torsional mode can be described as a hindered rotation of H_2O around the C_2 symmetry axis which also has the role of the principal b-axis for an isolated H_2O molecule. The torsional mode can as such be described as an almost genuine b-type rotation of H_2O although this motion is hindered in the complex. In the harmonic approximation the ratio of the two harmonic torsional band origins is thus proportional to the square root of the ratio of the B rotational constants for the two isotopic water molecules in question. In this way, the use of experimental B-values[26] predicts an isotopic harmonic red-shift of 21% for the band origin upon a single H/D-substitution. The model predicts a blue-shift of the proposed HDO torsional band origin at 128.4 cm^{-1} to 162.1 cm^{-1} for the corresponding IR-forbidden mode of the regular CO_2–H_2O system where our MP2 predictions provide a band origin close of 151.2 cm^{-1}. A complete unambiguous assignment of the HDO torsional cannot be justified solely by this crude model although the model provides a convincing argument. In our estimate for the zero-point energy we add a contribution of 75 ± 5 cm^{-1} from this IR-forbidden mode. The band origin of the medium intense CO_2 librational mode ν_{12} predicted to 16.8 cm^{-1} is close to the optical bandpass of our experimental setup and cannot be observed. In consequence, the zero-point energy contributions from this transition and the weak intermolecular O···C stretching transition ν_5 are based on the theoretical values listed in Table II. We estimate a total (semi)-empirical contribution to the zero-point energy from the class of intermolecular van der Waals transitions to 273 ± 15 cm^{-1} based on the present findings. A total zero-point energy contribution of 278 ± 15 cm^{-1} is achieved by inclusion of the predicted contribution caused by perturbations of the intramolecular vibrational transitions.[14]

The excellent agreement between our harmonic MP2 predictions and the observed band origins of CO_2–H_2O embedded in solid neon matrices is rather surprising. Harmonic predictions usually overshoot the actual (anharmonic) band origins for large-amplitude vibrational modes associated with intermolecular van der Waals transitions of weakly bound cluster molecules. A recent review addressing complexes of H_2O embedded in neon matrices reports that large-amplitude intermolecular vibrational transitions tend to be slightly blue-shifted relative to the gas phase although numerous red-shifts have been reported as well.[21] These small blue-shifts of large-amplitude vibrations are ascribed as minor repulsive steric effects originating from the congested neon host environment. These combined arguments could suggest that both our harmonic predictions and observed neon matrix band origins are slightly higher than expected gas-phase values. The present experimental findings thus invite for future high-level anharmonic theoretical investigations of the large-amplitude vibrational CO_2–H_2O motion which may shed light on the subtle balance of potential neon matrix blue-shifts and anharmonicity effects for this weakly bound system. We consider as such our current (semi)-empirical estimate of 273 ± 15 cm^{-1} as an upper limit for the intermolecular part of the zero-point energy. In the recent comprehensive theoretical study of the CO_2–H_2O system the highest level of theory including the almost complete electron correlation effects captured by the CCSD(T) approach and basis set superposition errors predicts an equilibrium dissociation energy D_e of 1004 cm^{-1}.[14] The combination with the present experimental findings thus provides a lower limit of 726 ± 15 cm^{-1} for the dissociation energy D_0 for this prototypical van der Waals interaction.

We appreciate the help and discussions with B. Brink, K. L. Feilberg, J. Ceponkus, A. Engdahl, and P. Uvdal. R.W.L.

acknowledges financial support from the Danish Council for Independent Research's Sapere Aude Programme (Grant No. 12-125248).

[1]R. R. Gamache, A. L. Laraia, and J. Lamouroux, Icarus **213**(2), 720–730 (2011).
[2]M. T. Nguyen, M. H. Matus, V. E. Jackson, V. T. Ngan, J. R. Rustad, and D. A. Dixon, J. Phys. Chem. A **112**(41), 10386–10398 (2008).
[3]Y. Abashkin, F. Mele, N. Russo, and M. Toscano, Int. J. Quantum Chem. **52**(4), 1011–1015 (1994).
[4]J. Altmann and T. Ford, J. Mol. Struct. **818**(1–3), 85–92 (2007).
[5]R. J. Wheatley and A. H. Harvey, J. Chem. Phys. **134**(13), 134309 (2011).
[6]J. Sadlej and P. Mazurek, J. Mol. Struct. **337**(2), 129–138 (1995).
[7]J. Sadlej, J. Makarewicz, and G. Chalasinski, J. Chem. Phys. **109**(10), 3919–3927 (1998).
[8]C. N. Ramachandran and E. Ruckenstein, Comput. Theor. Chem. **966**(1–3), 84–90 (2011).
[9]K. M. de Lange and J. R. Lane, J. Chem. Phys. **134**(3), 034301 (2011).
[10]M. Kieninger and O. Ventura, J. Mol. Struct. **390**, 157–167 (1997).
[11]Y. Danten, T. Tassaing, and M. Besnard, J. Phys. Chem. A **109**(14), 3250–3256 (2005).
[12]A. S. Tulegenov, Chem. Phys. Lett. **505**(21–23), 71–74 (2011).
[13]J. Makarewicz, T.-K. Ha, and A. Bauder, J. Chem. Phys. **99**(5), 3694–3699 (1993).
[14]J. Makarewicz, J. Chem. Phys. **132**(23), 234305 (2010).
[15]K. I. Peterson and W. Klemperer, J. Chem. Phys. **80**(6), 2439–2445 (1984).
[16]G. Columberg, A. Bauder, N. Heineking, W. Stahl, and J. Makarewicz, Mol. Phys. **93**(2), 215–228 (1998).
[17]L. Fredin, B. Nelander, and G. Ribbegard, Chem. Scr. **7**(1), 11–13 (1975).
[18]A. Schriver, L. Schriver-Mazzuoli, P. Chaquin, and E. Dumont, J. Phys. Chem. A **110**(1), 51–56 (2006).
[19]X. Zhang and S. P. Sander, J. Phys. Chem. A **115**(35), 9854–9860 (2011).
[20]J. Ceponkus, P. Uvdal, and B. Nelander, J. Chem. Phys. **129**(19), 194306 (2008).
[21]J. Ceponkus, A. Engdahl, P. Uvdal, and B. Nelander, Chem. Phys. Lett. **581**, 1–9 (2013).
[22]J. Ceponkus and B. Nelander, J. Phys. Chem. A **108**(31), 6499–6502 (2004).
[23]J. Ceponkus, P. Uvdal, and B. Nelander, J. Chem. Phys. **133**(7), 074301 (2010).
[24]J. Ceponkus, P. Uvdal, and B. Nelander, J. Phys. Chem. A **114**(25), 6829–6831 (2010).
[25]R. Bukowski, J. Sadlej, B. Jeziorski, P. Jankowski, K. Szalewicz, S. Kucharski, H. Williams, and B. Rice, J. Chem. Phys. **110**(8), 3785–3803 (1999).
[26]W. Benedict, N. Gailar, and E. K. Plyler, J. Chem. Phys. **24**(6), 1139 (1956).
[27]Y. Zhu, S. Li, P. Sun, and C. Duan, J. Mol. Spectrosc. **283**, 7–9 (2013).